THE JOURNAL OF BIOLOGICAL CHEMISTRY VOL. 287, NO. 5, pp. 3530–3540, January 27, 2012

Transient Receptor Potential Channel 1 (TRPC1) Reduces Calcium Permeability in Heteromeric Channel Complexes[S]

Received for publication, July 15, 2011, and in revised form, December 7, 2011 Published, JBC Papers in Press, December 8, 2011, DOI 10.1074/jbc.M111.283218

Ursula Storch[‡], Anna-Lena Forst[‡], Maximilian Philipp[§], Thomas Gudermann[‡1], and Michael Mederos y Schnitzler[‡]

From the [‡]Walther-Straub-Institute for Pharmacology and Toxicology, Ludwig-Maximilians University, 80336 Munich, Germany and the [§]Institute for Pharmacology and Toxicology, Marburg University, 35032 Marburg, Germany

Specific biological roles of the classical transient receptor potential channel 1 (TRPC1) are still largely elusive. To investigate the function of TRPC1 proteins in cell physiology, we studied heterologously expressed TRPC1 channels and found that recombinant TRPC1 subunits do not form functional homomeric channels. Instead, by electrophysiological analysis TRPC1 was shown to form functional heteromeric, receptor-operated channel complexes with TRPC3, -4, -5, -6, and -7 indicating that TRPC1 proteins can co-assemble with all members of the TRPC subfamily. In all TRPC1-containing heteromers, TRPC1 subunits significantly decreased calcium permeation. The exchange of select amino acids in the putative pore-forming region of TRPC1 further reduced calcium permeability, suggesting that TRPC1 subunits contribute to the channel pore. In immortalized immature gonadotropin-releasing hormone neurons endogenously expressing TRPC1, -2, -5, and -6, down-regulation of TRPC1 resulted in increased calcium permeability and elevated basal cytosolic calcium concentrations. We did not observe any involvement of TRPC1 in store-operated cation influx. Notably, TRPC1 suppressed the migration of gonadotropin-releasing hormone neurons without affecting cell proliferation. Conversely, in TRPC1 knockdown neurons, specific migratory properties like distance covered, locomotion speed, and directionality were increased. These findings suggest a novel regulatory mechanism relying on the expression of TRPC1 and the subsequent formation of heteromeric TRPC channel complexes with reduced calcium permeability, thereby fine-tuning neuronal migration.

The classical transient receptor potential (TRPC)[2] channel subfamily comprises seven members (TRPC1–7) that are regarded as non-selective, calcium-permeable cation channels involved in a wide range of physiological events that require calcium (Ca^{2+}) signaling. To date, it is broadly accepted that the general activation mechanism of TRPC channels is contingent upon receptor-mediated phospholipase C activation independent of protein kinase C activity and the depletion of internal calcium stores (1). However, channel activation subsequent to store depletion is also discussed for some TRPC family members (summarized by Ref. 2). TRPC channels are widely expressed in different mammalian tissues like vascular smooth muscle, lung, kidney, and brain, and they have been identified to participate in central cell physiological processes (3). In the nervous system, for example, TRPC channels are involved in neuronal development, proliferation, and differentiation (4, 5), and a growing body of evidence indicates that TRPC channels are involved in neurological diseases (6).

For TRPC1 channels, an involvement in stretch-induced (7) and in store-operated calcium (SOC) influx is discussed (8–10). Previous investigations of TRPC1 gene-deficient mice indicated that TRPC1 was neither involved in store-operated cation influx in vascular smooth muscle cells and in platelets (11, 12) nor in pressure-induced cation influx (11). However, a contribution of TRPC1 to SOC in neurons is still a moot issue. Moreover, a detailed analysis of the specific role of TRPC1 for receptor-operated calcium influx in neurons has not been conducted.

Although numerous publications demonstrate that TRPC1 channels are involved in many intracellular processes like smooth muscle contraction, stem cell differentiation and endothelial cell permeability, salivary gland secretion, growth cone movement, neuronal differentiation, and glutamate-mediated neurotransmission (8, 9, 13), TRPC1 gene-deficient mice did not exhibit an obvious phenotype (11). Furthermore, the specific role of TRPC1 channels for neuronal migration in the developing brain is still elusive.

Based on the finding that TRPC1 is able to form receptor-operated heterotetrameric channel complexes with other TRPC channel subunits (14), we investigated the role of TRPC1 alone and in heteromeric channel complexes for receptor-operated calcium influx in a heterologous expression system as well as in neurons. We observed that upon incorporation into heteromeric channel complexes TRPC1 subunits contribute to the channel pore and decrease calcium permeation. As a consequence the presence of TRPC1 in immortalized immature GnRH neurons suppresses neuronal migration without affecting cell proliferation, thus highlighting a novel regulatory mechanism based on the formation of heteromeric TRPC channel complexes with reduced calcium permeability.

EXPERIMENTAL PROCEDURES

Cell Culture—Human embryonic kidney (HEK293) cells were maintained in Earl's minimal essential medium (Invitrogen), CHO-K1 cells were cultured in Ham's F-12 medium (Invitrogen), and immortalized murine gonadotropin releasing

[S] This article contains supplemental Figs. S1–S7.

[1] To whom correspondence should be addressed: Walther-Straub-Institute for Pharmacology and Toxicology, Ludwig-Maximilians University, Goethestrasse 33, 80336 Munich, Germany. Tel.: 49-89-218075700; Fax: 49-89-218075701; E-mail: thomas.gudermann@lrz.uni-muenchen.de.

[2] The abbreviations used are: TRPC, transient receptor potential; SOC, store-operated calcium; GnRH, gonadotropine releasing hormone; qPCR, quantitative real-time PCR; M_5R, muscarine M_5 receptor; CCh, carbachol; EGFP, enhanced GFP; GTPγS, guanosine 5′-3-*O*-(thio)triphosphate.

hormone (GnRH) neurons (Gn11 cells) (15) were maintained in Dulbecco's modified Eagle's medium (DMEM, Invitrogen) supplemented with 10% fetal calf serum (FCS, Invitrogen), 100 units ml^{-1} penicillin, and 100 $\mu g\ ml^{-1}$ streptomycin and 2 mM glutamine at 37 °C in a humidified atmosphere with 5% CO_2. Monoclonal TRPC1 knockdown and control Gn11 cell lines were cultured in DMEM additionally containing 800 $\mu g\ ml^{-1}$ Geneticin (Invitrogen).

Mutagenesis—For amino acid exchanges from glutamate to glutamine at positions 581 and 582, mutations in TRPC1 were introduced by site-directed mutagenesis using the QuikChange system (Stratagene, La Jolla, CA). All cDNA constructs used in the present work were confirmed by sequencing.

Generation of shRNA—To investigate the role of TRPC1 in Gn11 cells, RNA interference was used (16). For this, shRNA was transiently expressed via a pSuper NeoGFP expression vector. shRNA targeting murine TRPC1, murine TRPC5 and murine TRPC6 was designed according to Reynolds *et al.* (17) with additional testing of the three-dimensional structure of the mRNA target sequence to ensure optimal efficacy of RNA interference (18). As a control, unrelated shRNA was expressed. The DNA sequence was 5′-ACT TAA GTC GTC TGA AAC T-3′ for the TRPC1-specific construct, 5′-ATC AAA TAT CAC CAG AAA G-3′ for the TRPC5-specific construct, 5′-TCG AGG ACC AGC ATA CAT G-3′ for the TRPC6-specific construct, and 5′-TTT GAT TTG CGA AGG TTT T-3′ for the unrelated construct. shRNA constructs targeting TRPC5 and TRPC6 were expressed employing a pSuper NeoGFP expression vector with GFP being exchanged to JRed by subcloning. For transient transfections, either TransIT (Mirus Bio LLC, Madison) or the NEON device (Invitrogen) was used according to the manufacturer's protocol. The efficiency of the shRNA construct was tested using quantitative real-time polymerase chain reaction and Western blot analysis. All shRNA constructs used had no effect on the TRPC expression profile of Gn11 cells.

Quantitative Real-time Polymerase Chain Reaction (qPCR) Analysis—Total RNA from Gn11 cells was isolated using the Tri Reagent (Sigma). First-strand synthesis was carried out with random hexamers as primers using REVERTAID reverse transcriptase (Fermentas, Sankt Leon-Roth, Germany). The following primers pairs were used for the amplification of specific fragments from the first-strand synthesis: TRPC1, C1for (5′-GAT GTG TCT TTG CCC AAG C-3′), C1rev (5′-CTG GAC TGG CCA GAC ATC TAT-3′), TRPC2, C2for (5′-ACT TCA CTA CAT ATG ATC TGG GTC AC-3′), C2rev (5′-CAC GTC CAG GAA GTT CCA C-3′), TRPC3, C3for (5′-TTA ATT ATG GTC TGG GTT CTT GG-3′), C3rev (5′-TCC ACA ACT GCA CGA TGT ACT-3′), TRPC4, C4for (5′-AAG GAA GCC AGA AAG CTT CG-3′), C4frev (5′-CCA GGT TCC TCA TCA CCT CT-3′), TRPC5, C5for (5′-GCT GAA GGT GGC AAT CAA AT-3′), C5rev (5′-AAG CCA TCG TAC CAC AAG GT-3′), TRPC6, C6for (5′-ACT GGT GTG CTC CTT GCA G-3′), C6rev (5′-GAG CAG CCC CAG GAA AAT-3′), TRPC7, C7for (5′-CCC AAA CAG ATC TTC AGA GTG A-3′), C7rev (5′-TGC ATT CGG ACC AGA TCA T-3′), voltage-gated N-type calcium channel, $Ca_vN$for (5′-CCA GGA ACC TCC TTT GGA AT-3′), Ca_vNrev (5′-AAA CCA CCA GGT TCC TCA GA-3′), voltage-gated PQ-type calcium channel, $Ca_vPQ$for (5′-CTG ACA TCG CGT CTG TGG-3′), Ca_vPQrev (5′-CGC ATT CTT CTC TCC TTC TTG-3′), and three references, hypoxanthin phosphoribosyltransferase 1, Hprt1for (5′-TCC TCC TCA GAC CGC TTT T-3′), Hprt1rev (5′-CCT GGT TCA TCA TCG CTA ATC-3′), tyrosine 3-monooxygenase/tryptophan 5-monooxygenase activation protein, ζ-polypeptide, Ywhazfor (5′-TAA AAG GTC TAA GGC CGC TTC-3′), Ywhazrev (5′-CAC CACA CGC ACG ATG AC-3′), and succinate dehydrogenase complex, subunit A, Sdhafor (5′-CCC TGA GCA TTG CAG AAT C-3′), Sdharev (5′-TCT TCT CCA GCA TTT GCC TTA-3′) giving predicted product sizes of 127 bp for TRPC1, 111 bp for TRPC2, 91 bp for TRPC3, 92 bp for TRPC4, 90 bp for TRPC5, 101 bp for TRPC6, 94 bp for TRPC7, 100 bp for Ca_vN, 100 bp for Ca_vPQ, 90 bp for Hprt1, 60 bp for Ywhaz, and 70 bp for Sdha. Real-time polymerase chain reaction (RT-PCR) was performed using the master mix from the Absolute QPCR SYBR Green Mix kit (Abgene, Epsom, UK). Ten picomoles of each primer pair and 0.2 μl of the first-strand synthesis was added to the reaction mixture, and PCR was carried out in a light-cycler apparatus (Light-Cycler 480, Roche Applied Science) using the following conditions: 15 min of initial activation and 45 cycles of 12 s at 94 °C, 30 s at 50 °C, 30 s at 72 °C, and 10 s at 80 °C each. Fluorescence intensities were recorded after the extension step at 80 °C after each cycle to exclude fluorescence of primer dimers melting lower than 80 °C. All primers were tested by using diluted complementary DNA (cDNA) from the first-strand synthesis (10–1000×) to confirm linearity of the reaction and to determine particular efficiencies. Data were calculated as percentage of mean expression of the three references. Samples containing primer dimers were excluded by melting curve analysis and identification of the products by agarose gel electrophoresis. Crossing points were determined by the software program. All experiments were performed in quadruplets, and experiments were repeated at least three times.

Detection of TRPC1 Protein—To confirm the efficiency of TRPC1 shRNA, CHO-K1 cells were stably transfected with HA-tagged mouse TRPC1 (NM_011643). Cells were transiently transfected with different shRNAs using the NEON device (Invitrogen) as described by the manufacturer. Two days after transfection, cells were lysed for 10 min in radioimmune precipitation assay buffer (50 mM Tris, pH 7.5, 200 mM NaCl, 1% Triton X-100, 0.25% deoxycholate, 1 mM EDTA, 1 mM EGTA, and freshly added protease inhibitors (Fermentas)) on ice and centrifuged for half an hour at maximum speed. Supernatant was placed in SDS sample buffer, boiled for 5 min, and subjected to gel electrophoresis on a 12% SDS-PAGE gel. Proteins were transferred onto PVDF membranes as described by manufacturer (Bio-Rad). After transfer, blots were blocked with 1× RotiBlock (Roth, Karlsruhe, Germany) and incubated with primary mouse anti-HA (Sigma) or mouse anti-GAPDH antibody (Sigma) in combination with secondary anti-mouse antibody (Promega, Mannheim, Germany) to determine the expression of TRPC1. The experiment was repeated three more times with comparable results.

Electrophysiology—HEK293 cells were transfected with cDNAs coding for human TRPC1 (NM_003304), TRPC3 (NM_001130698), TRPC6 (NM_004621), and TRPC7 (NM_

020389), mouse TRPC5 (NM_009428), and rat TRPC4β1 (NM_001083115) with the original cDNA coding for the rat type-5 muscarinic (M_5R) acetylcholine receptor in pcDNA3 using TransIT (Mirus Bio LLC) reagent unless mentioned otherwise. TRPC1 in pcDNA3 and in pRK5 (Genentech) with an N-terminal HA-tag and TRPC3 and TRPC7 in pcDNA3 were additionally co-transfected with the enhanced green fluorescent protein (EGFP) reporter plasmid. TRPC1, TRPC4β1, TRPC5, and TRPC6 were also present in pIRES2-EGFP (Clontech, Palo Alto, CA). Gn11 cells were either transiently transfected with shRNA against TRPC1 or unrelated control shRNA or were used as stable shRNA against TRPC1 or unrelated shRNA-expressing cells. Conventional whole-cell patch clamp recordings were carried out at 23 °C 48 h after transfection. Cells were superfused with the standard bath solution (Na^+_{div}) containing 140 mM NaCl, 5 mM CsCl, 1 mM $MgCl_2$, 2 mM $CaCl_2$, 10 mM glucose, 10 mM HEPES (pH 7.4 with NaOH) supplemented with mannitol to 300 mosmol kg^{-1}. Gn11 cells were superfused with the standard bath solution plus 50 μM 5-nitro-2-(3-phenyl-propylamino)-benzoate to suppress chloride conductance. For the determination of calcium permeabilities, a divalent-free sodium extracellular solution (Na^+, 130 mM NaCl, 50 mM mannitol, and 10 mM HEPES, pH 7.4) and a monovalent-free calcium solution (Ca^{2+}, 10 mM $CaCl_2$ and 150 mM *N*-methyl-D-glucamine-Cl, pH 7.4) were applied. The protocol for whole-cell measurements was the following; 1) superfusion with $Na^+_{div,}$ solution, 2) when current activation occurred, application of Ca^{2+} solution for 60 s, and 3) application of Na^+ solution. In the case of receptor stimulation, 100 μM carbachol was added in Na^+_{div}, in Ca^{2+}, and in Na^+ solution. Permeability ratios (P_{Ca}/P_{Na}) were determined using the following equation (19),

$$\frac{P_{div}}{P_{Na}} = \frac{e^{((RP_{div} - RP_{Na})\,R^{-1}T^{-1}F)}\,[Na]_o\,(1 + e^{(RP_{div}\,R^{-1}T^{-1}F)}}{4[div]_o} \qquad \text{(Eq. 1)}$$

where $[Na]_o$ represents the extracellular sodium ion concentration, $[div]_o$ represents the extracellular calcium concentration, RP_{Na} represents the reversal potential (E_{rev}) of the sodium current, RP_{div} represents the E_{rev} of the calcium current, *R* represents the gas constant, *T* represents the absolute temperature, and *F* represents the Faraday constant.

The pipette solution contained 130 mM cesium methanesulfonate, 10 mM CsCl, 9.4 mM NaCl, 0.2 mM Na_3GTP, 1 mM $MgCl_2$, 3.949 mM $CaCl_2$, 10 mM BAPTA (100 nM free Ca^{2+}), and 10 mM HEPES (pH 7.2 with CsOH), resulting in an osmolality of 294 mosmol kg^{-1}. Data were collected with an EPC10 patch clamp amplifier (HEKA, Lambrecht, Germany) using the Pulse software. Current voltage relations were obtained from triangular voltage ramps from −100 to +60 mV with a slope of 0.4 V s^{-1} applied at a frequency of 1 Hz. Data were acquired at a frequency of 5 kHz after filtering at 1.67 kHz. The IV curves and the current amplitudes were always extracted at maximal currents.

Determination of Intracellular Calcium Concentrations and Mn^{2+} Quenching—Intracellular free calcium was determined in Gn11 cells and Gn11 cells stably expressing shRNA against TRPC1 or unrelated control shRNA. Cells were loaded for 15–30 min with fura-2-acetoxymethyl ester (5 μM; Molecular Probes Inc., Eugene, OR) in HEPES-buffered saline containing 140 mM NaCl, 5 mM KCl, 1 mM $MgCl_2$, 2 mM $CaCl_2$, 5 mM glucose, 10 mM HEPES (pH 7.4 with NaOH) at 37 °C. Coverslips were mounted on the stage of a monochromator-equipped (Polychrome V, TILL-Photonics, Martinsried, Germany) inverted microscope (Olympus IX 71 with an UPlanSApo 20×/0.85 oil immersion objective). Fluorescence was recorded with a 14-bit EMCCD camera (iXON3 885, Andor, Belfast, UK). Fura-2 fluorescence was excited at 340 and 380 nm. Intracellular free calcium concentrations were calculated as described previously (20). For imaging experiments, Gn11 cells were seeded on coverslips. Cells were continuously superfused at room temperature with HEPES-buffered saline. For store depletion experiments, Gn11 cells were superfused with calcium-free HEPES-buffered saline containing 2 mM EGTA and 10 μM cyclopiazonic acid for at least 10 min. Subsequently HEPES-buffered saline containing 2 mM Ca^{2+} and 10 μM cyclopiazonic acid was added, and calcium influx was monitored. Finally 5 μM Gd^{3+} was added to block unselective cation channels.

Mn^{2+} quench experiments were conducted 48 h after transfection of HEK293 cells. Transfected HEK293 cells were loaded for 30 min with fura-2-acetoxymethyl ester in HEPES-buffered saline. The fluorescence of fura-2 and enhanced yellow fluorescence protein was excited at 340, 360, 380, and 500 nm. Fura-2 was not excited at 500 nm, and enhanced YFP contributed negligibly to fluorescence excited at 340–380 nm. Cells were continuously superfused at room temperature with HEPES-buffered saline. In Mn^{2+} quench experiments, 200 μM $MnCl_2$ was applied. Mn^{2+} quench was calculated and normalized as described previously (21).

Scratch Assay—Gn11 cells were stably transfected with TRPC1 and control shRNA. Down-regulation of TRPC1 was confirmed with qPCR. To analyze motility of Gn11 cells, 5×10^5 cells were plated in DMEM plus 10% FCS in a 10-cm plastic dish at least 32 h before the experiment. To initiate migration of cells, the cell layer was scratched six times per well with a yellow pipette tip and marked with a perpendicular line on the outside of the dish. Dishes were washed twice with PBS, then normal growth medium was gently added. A picture of the scratch was taken at 5× magnification using an inverse microscope (Axiovert 40 CFL, Zeiss, Göttingen, Germany) immediately after and 16 h after scratch. Migrated cells were counted using the ImageJ software. All experiments were carried out at least in triplicate, and all results are reported as -fold increase of migrated cells compared with control Gn11 cells stably expressing unrelated shRNA.

Videomicroscopy—20.000–40.000 Gn11 cells stably transfected with shRNA against TRPC1 or control shRNA were seeded in 35-mm culture dishes with glass bottoms (FluoroDish, WPI, Berlin, Germany) 24 h before the experiment. Dishes were mounted on an inverse microscope (Axiovert 40 CFL, Zeiss). Using a digital camera (AxioCamICc1, Zeiss) with the AxioVision 4.8.2 software (Zeiss), movies of Gn11 cells were acquired at a 10× magnification by shooting single photographs every 30 s for a period of 16 h. During the experiments, cells were maintained in culture medium and held at 37 °C in a

humidified atmosphere with 5% CO_2. Analysis of the migratory properties was done with the AxioVision software.

G-actin/F-actin Assay—We used Western blot quantification to determine the amount of filamentous actin (F-actin) *versus* free globular actin (G-actin) as described previously (22). Briefly, 300,000 Gn11 cells stably transfected with either shRNA against TRPC1 or control shRNA were seeded in a 6-well dish 1 day before harvesting cells at 37 °C with 750 μl of freshly prepared lysis buffer (50 mM PIPES, pH 6.9, 50 mM NaCl, 5 mM $MgCl_2$, 5 mM EGTA, 5% (v/v) glycerol, 0.1% Nonidet P40, 0.1% Triton X-100, 0.1% Tween 20, 0.1% 2-mercaptoethanol, 0.001% Antifoam C, 1 mM ATP, and protease inhibitor mixture (Fermentas)). Lysis buffer for the F-actin-positive control sample additionally contained 1 μM phalloidin (Sigma), whereas the G-actin positive control sample contained 10 μM cytochalasin D (Sigma). Cells were incubated for 10 min at 37 °C and centrifuged for 5 min at 2000 rpm to pellet unbroken cells. The homogenate was ultracentrifuged at 100,000 × *g* for 1 h at 37 °C. After centrifugation, the supernatant containing soluble G-actin was transferred to a new tube, whereas the pellet containing the F-actin fraction was resuspended to the same volume as the supernatant using ice-cold water plus 10 μM cytochalasin D and left on ice for 1 h to dissociate F-actin. Samples were analyzed using SDS-PAGE electrophoresis, blotted onto a PVDF membrane, and analyzed with anti-actin antibody (Sigma).

Statistical Analysis—Data are presented as the S.E. Unless stated otherwise, data were compared by a paired or unpaired Student's *t* test if a Gaussian distribution was confirmed by applying a Shapiro-Wilk (normality) test, and significance was accepted at $p < 0.05$. *, $p < 0.05$; **, $p < 0.01$; ***, $p < 0.001$, *n.s.*, $p > 0.05$.

RESULTS

TRPC1 Suppresses Calcium Permeability in Heteromeric Channel Complexes with TRPC4 and -5 but Is Not Able to Form Functional Receptor-operated Homomeric Channels—To investigate whether TRPC1 is able to form functional homomeric channel complexes, we first used a heterologous expression system and performed patch clamp recordings in the whole-cell configuration with HEK293 cells overexpressing recombinant TRPC1 and the G_q-protein-coupled muscarinic M_5 receptor (M_5R). Receptor activation by carbachol (100 μM) in the bath solution (Fig. 1, *A* and *B*) as well as by GTPγS (200 μM) infusion through the patch pipette (supplemental Fig. S1, *A* and *B*) failed to activate cation currents in TRPC1 overexpressing HEK293 cells. Current densities at ±60 mV and current-voltage relationships (IVs) were not different between TRPC1-expressing and control cells (EGFP and receptor co-expressing and untransfected HEK293 cells). Identical observations were made when recombinant TRPC1 was expressed in CHO-K1 cells (supplemental Fig. S1, *D* and *E*). To obtain more detailed information about the biophysical properties of TRPC1 overexpressing cells, we analyzed ion permeabilities using an external solution containing 10 mM Ca^{2+}. However, calcium permeability in TRPC1 overexpressing cells did not differ from control cells (Fig. 1*C* and supplemental Fig. S1*C*). Because it has been reported that reduction of the phosphatidylinositol 4,5-bisphosphate content of the plasma membrane activates certain TRPC channels (23, 24), we analyzed whether TRPC1 is also regulated by phosphatidylinositol 4,5-bisphosphate depletion using wortmannin (20 μM), an inhibitor of phosphoinositide 3-kinases causing phosphatidylinositol 4,5-bisphosphate depletion at high concentrations. Incubation with wortmannin had no effect on endogenous cation currents and did not change the calcium permeability of TRPC1-expressing cells as compared with untransfected cells (supplemental Fig. S1, *F–H*). Taken together, these findings indicate that homomeric recombinant TRPC1 is incapable of forming functional receptor-operated channels despite its high mRNA expression level (supplemental Fig. S2).

Because co-expression of TRPC1 together with TRPC4 or TRPC5 results in receptor-operated heteromeric channel complexes with characteristic channel properties (25), we sought to define the specific contribution of TRPC1 to the biophysical properties of heteromeric channel complexes. Co-expression of TRPC1 with TRPC4 or TRPC5 and M_5R in HEK293 cells resulted in rapidly developing inward and outward currents evoked by agonist stimulation with carbachol or by GTPγS infusions showing altered biophysical properties compared with cells expressing TRPC4 or TRPC5 alone (Fig. 1, *D* and *E*). In physiological bath solution current voltage curves exhibited significantly larger outward and smaller inward currents mirrored by increased current ratios at ±60 mV (Fig. 1*F*). Furthermore, in a bath solution containing 10 mM Ca^{2+}, reversal potentials of heteromeric channels were significantly shifted toward more negative potentials, indicating that TRPC1 reduces the calcium permeability of heteromeric channel complexes containing TRPC4 and TRPC5 (Fig. 1, *G–I*).

TRPC1 Is Pore-forming Subunit in Heteromeric Channel Complexes and Reduces Calcium Permeabilities When Co-assembled with TRPC3/6 and -7—Next, we investigated whether co-expression with TRPC1 would also modify channel properties of the members of the diacylglycerol-sensitive subfamily TRPC3, -6, and -7. Notably, receptor-activated currents in TRPC3/1 and TRPC7/1 and M_5R co-expressing cells were characterized by significantly increased ratios of outward to inward currents at ±60 mV when compared with cells expressing TRPC3 or TRPC7 and M_5R (Fig. 2, *A* and *C*). In addition, slope conductances at ±55 mV (determined at current amplitudes of −200 pA and +1 nA) were significantly different. In physiological bath solution no differences were observed between TRPC6/1- and TRPC6-expressing cells (Fig. 2*B*) although both TRPC subunits were highly expressed at the mRNA level (supplemental Fig. S2). However, application of 10 mM Ca^{2+} to the bath always resulted in a leftward shift of reversal potentials of TRPC1-co-expressing cells reflecting a significantly reduced calcium permeability (Fig. 2, *E* and *F*) that was not noted in TRPM7/TRPC1-co-expressing cells (supplemental Fig. S3). These findings indicate a potential function of TRPC1 as a modulator of calcium permeabilities of heteromeric TRPC channel complexes.

To sort out the mechanism by which TRPC1 alters calcium permeabilities, we asked whether TRPC1 functions as a pore-forming subunit in heteromeric channel complexes. Amino acid exchanges from glutamate to glutamine at positions 581 and 582 in the putative pore region of TRPC1 resulted in a

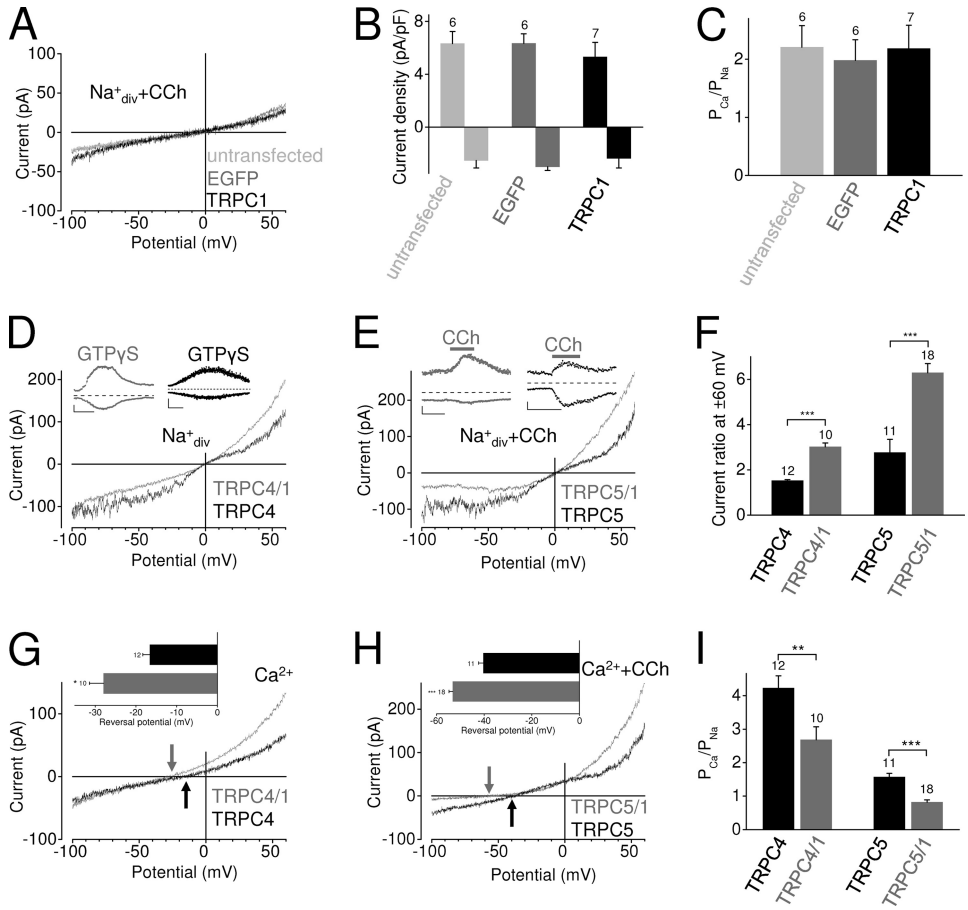

FIGURE 1. **TRPC1 attenuates calcium permeability in heteromeric channel complexes with TRPC4 and 5, but TRPC1 *per se* cannot form functional receptor-operated homomeric channel complexes.** *A–I*, shown are whole-cell recordings from untransfected HEK293 cells and HEK293 cells expressing EGFP alone or TRPC1 and the muscarinic M_5R (*A–C*) or expressing TRPC4 or TRPC5 alone or in combination with TRPC1 and M_5R (*D–I*). TRPC4-expressing cells were activated by infusions of 200 μM GTPγS through the patch pipette (*D*) and TRPC5-expressing cells by receptor stimulations with 100 μM carbachol (*E*). Exemplary IV curves in standard bath solution (Na^+_{div}) (*D*) and (Na^+_{div}+*CCh*) (*A* and *E*) and in 10 mM Ca^{2+} solution (Ca^{2+}) (*G*) and in (Ca^{2+}+*CCh*) (*H*) are shown. *D* and *E*, *insets* in *D* and *E* show current time courses at ±60 mV, 0 current levels (*stippled lines*), *time scale bars* (100 s), and *current scale bars* (50 pA). *G* and *H*, *arrows* indicate reversal potentials. *Insets* in *G* and *H* show the analysis of reversal potentials determined in 10 mM Ca^{2+} solution. *B*, analysis of current densities at ±60 mV is shown. *C* and *I*, analysis of calcium permeabilities is shown. *F*, analysis of current ratios determined at holding potentials of ±60 mV is shown. indicate the number of cells measured. *pF*, picofarads; **, $p < 0.01$; ***, $p < 0.001$.

significantly reduced calcium permeability when co-expressed with TRPC5 (Fig. 2, *G* and *H*). This pair of glutamic acid residues is only present in the putative pore region of TRPC1 but not in other TRPCs. The simultaneous exchange of both glutamates had no additional effect. These findings indicate that in heteromeric channel complexes TRPC1 proteins are involved in the formation of the pore region. Moreover, to determine changes of cation permeability by a different approach, basal entry of extracellular divalent cations was analyzed by measuring the quenching of the fura-2 fluorescence by influx of extracellular Mn^{2+}. A pronounced quench of fura-2 fluorescence was observed in TRPC3-expressing cells (Fig. 2*I*), reflecting this channel high basal activity of about 50% (21). In TRPC3- and TRPC1-co-expressing cells, fura-2 quenching was significantly reduced, indicating a decrease of divalent cation influx. Co-expression of the TRPC1 mutant $TRPC1^{E582Q}$ reduced Mn^{2+} quenching even further demonstrating that under basal conditions cation entry through homomeric TRPC3 channels is significantly reduced in the presence of TRPC1. To test whether the reduced divalent cation influx in TRPC1-co-expressing cells was based on altered ion channel expression levels, we performed additional qPCR experiments (supplemental Fig. S4). mRNA expression levels of recombinant TRPC1 and TRPC3 were not significantly different, suggesting that the reduced divalent cation influx observed was most likely not caused by different TRPC expression levels. These findings affirm that TRPC1 is a pore-forming subunit in heteromeric TRPC channel complexes thereby reducing the calcium permeability.

TRPC1 Attenuates Calcium Permeability in GnRH Neurons Thereby Reducing Basal Intracellular Calcium Concentrations—We wondered whether endogenously expressed TRPC1 would also impact calcium permeation. To this end, immortalized murine GnRH-releasing neurons (Gn11 cells), originally derived from the olfactory bulb at embryonic state day 11.5, were investigated because they prominently express TRPC1 as detected by quantitative RT-PCR analysis (Fig. 3*A*). TRPC2, TRPC5, and TRPC6 were expressed less abundantly. In addition, the expression pattern of voltage-gated calcium channels (Ca_Vs) was examined showing that these neurons only express Ca_Vs of the PQ- but not of the N-type, most likely due to their immature nature. To define the specific role of TRPC1 in these

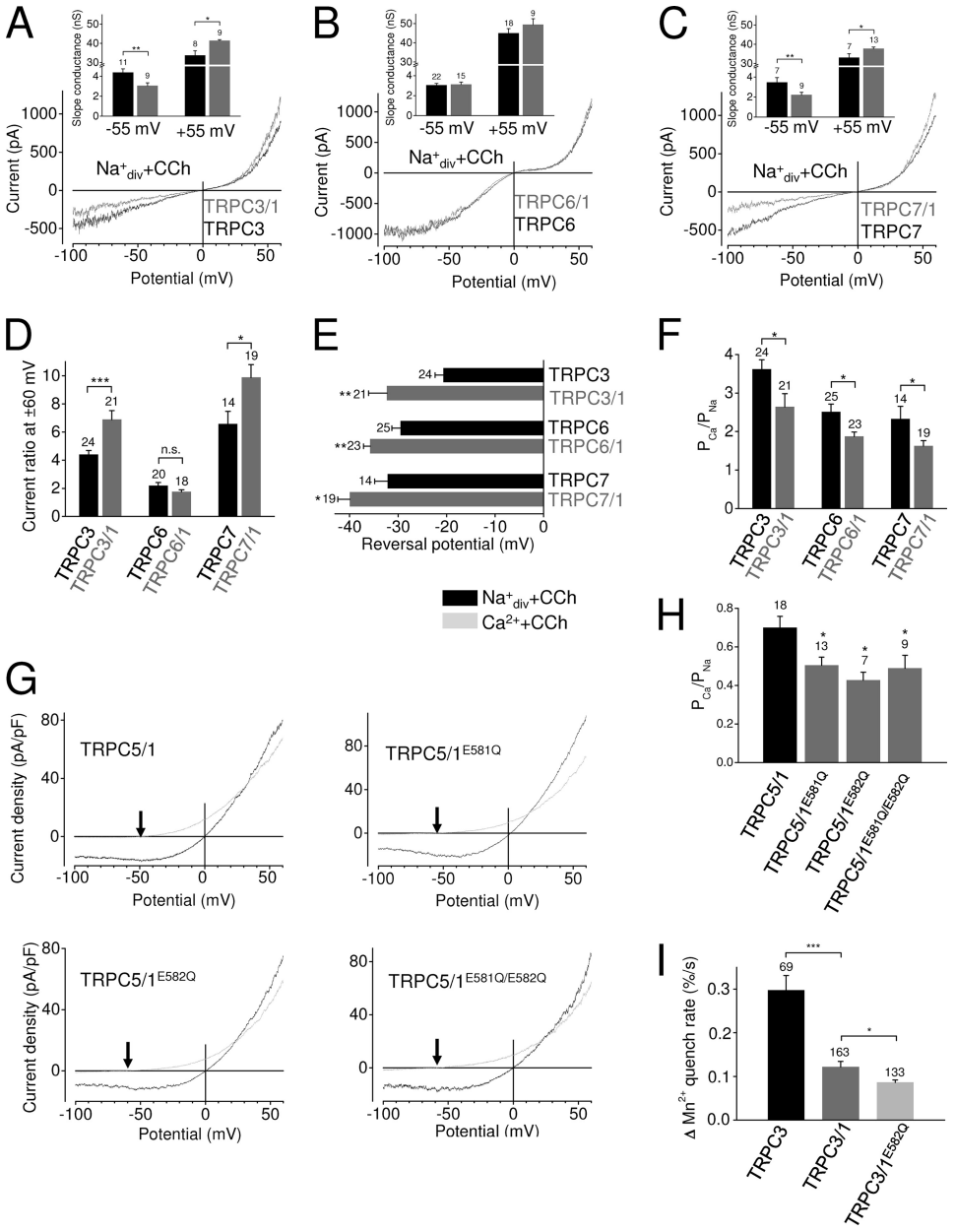

FIGURE 2. **TRPC1 is a pore-forming subunit in heteromeric channel complexes and suppresses the calcium permeability of TRPC3/6/7 channel complexes.** *A–H*, whole-cell recordings are shown of HEK293 cells expressing TRPC3, TRPC6, or TRPC7 alone or in combination with TRPC1 together with M_5R (*A–C*) or of HEK293 cells co-expressing TRPC5 and TRPC1 or TRPC1 mutant channels with amino acid exchanges from glutamate to glutamine at positions 581 (E581Q) and 582 (E582Q) or both (E581Q/E582Q) in combination with the M_5R (*G* and *H*). *A–C*, typical carbachol-induced IV curves measured in standard bath solution (Na^+_{div}+*CCh*) are displayed. *Insets* show the slope conductance determined during voltage changes from −50 to −60 mV (−55 mV) and from +50 to +60 mV (+55 mV). Only measurements with inwards currents of −200 ± 10 pA at −60 mV and outward currents of 1 ± 0.02 nA at +60 mV were included in the calculations. *nS*, nano Siemens. *D*, analysis of the ratios between outward and inward currents at ±60 mV is shown. *E*, analysis of the reversal potentials determined during application of 10 mM Ca^{2+} solution in the presence of carbachol is shown. *F*, analysis of the respective calcium permeabilities is shown. *G*, current density-voltage relationships of carbachol-induced currents in standard bath solution (Na^+_{div}+*CCh*) and in 10 mM Ca^{2+} solution (Ca^{2+}+*CCh*) are displayed. The *arrows* indicate the reversal potentials in Ca^{2+} solution in the presence of carbachol. *H*, shown is analysis of the calcium permeabilities. The *numbers over the bars* indicate the number of cells measured. *I*, analysis of Mn^{2+} quenching experiments with fura-2-loaded HEK293 cells expressing recombinant TRPC3 alone and TRPC3/TRPC1 as well as TRPC3/TRPC1^{E582Q} in the presence of 200 μM extracellular Mn^{2+}. Each indicated transfection shows the normalized Mn^{2+} quench rate expressed as percentages over time. *Numbers above the bars* indicate the number of cells measured of six independent experiments for each indicated transfection. *, $p < 0.05$; **, $p < 0.01$; ***, $p < 0.001$.

neuronal cells, channel expression was suppressed using an shRNA approach. TRPC1 expression was significantly reduced to 13.1 ± 9.4% by a specific shRNA directed against TRPC1 when compared with wild-type cells (Fig. 3*B*), whereas unrelated control shRNA had no effect on TRPC1 expression. Additionally, the efficiency of TRPC1 knockdown was tested on the protein level by Western blot analysis. Because of the lack of specific antibodies against endogenous TRPC1 proteins in Gn11 neurons, CHO-K1 cells stably expressing N- and C-terminal-tagged TRPC1 (HA-mTRPC1-HA) were used, and TRPC1 was detected by an anti-HA antibody. Transient transfections with shRNA against TRPC1 resulted in disappearance of the TRPC1 band, whereas the expression of control shRNA had no effect (Fig. 3*C*), demonstrating that the shRNA used

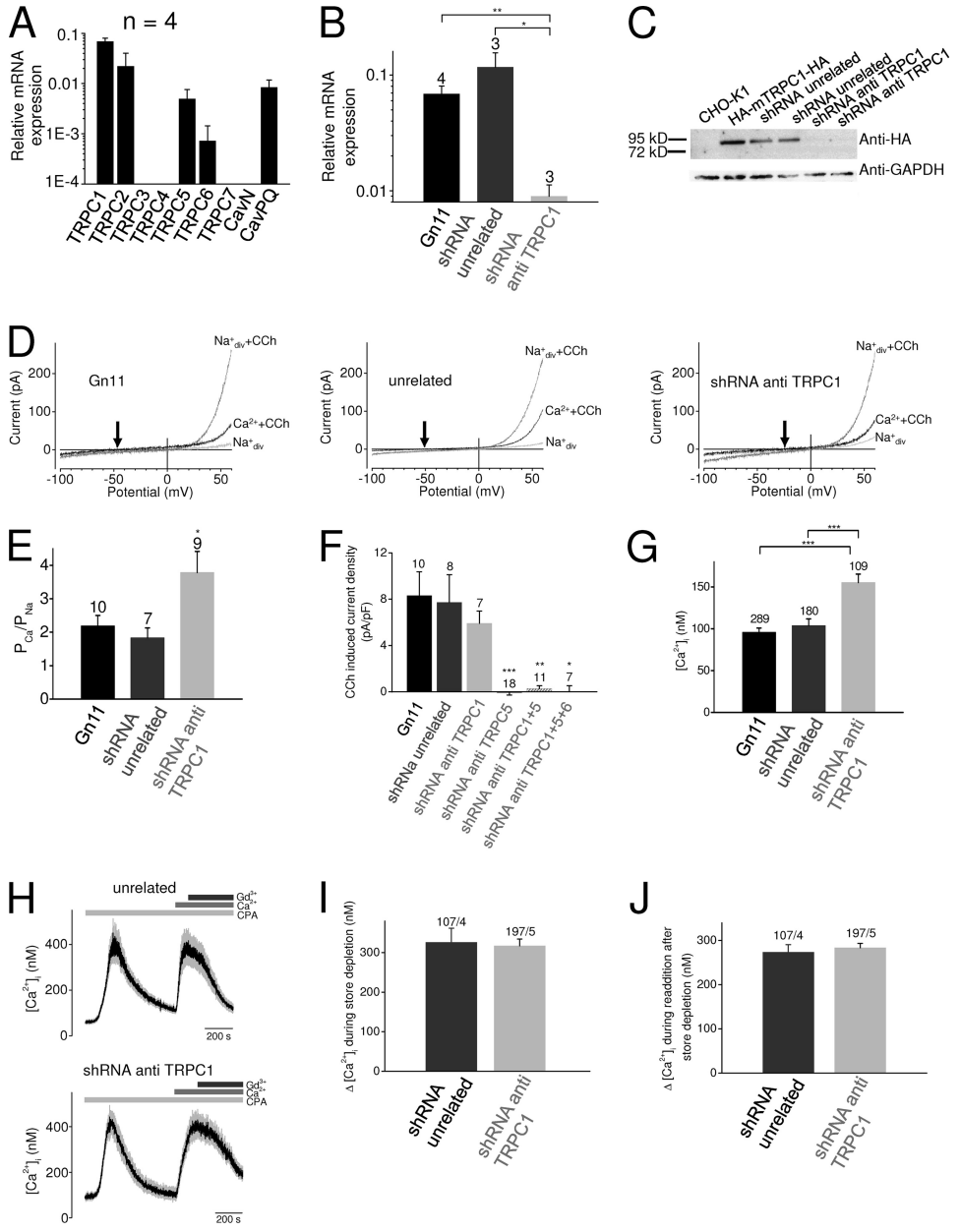

FIGURE 3. **TRPC1 reduces the calcium permeability and the cytosolic calcium concentrations in Gn11 neurons without affecting the store-operated calcium influx.** *A*, shown is relative mRNA expression analysis of TRPC channels and voltage-gated N-type and PQ-type calcium channels in Gn11 cells. *B*, analysis of the relative mRNA TRPC1 expression in Gn11 wild-type cells and in monoclonal Gn11 cell lines stably expressing unrelated control shRNA (*shRNA unrelated*) and shRNA targeting TRPC1 (*shRNA anti-TRPC1*). The *numbers over the bars* indicate the number of independent experiments each determined as quadruplets. *C*, Western blot analysis of CHO-K1 cells and of CHO-K1 cells stably expressing HA-tagged TRPC1 (*CHO-K1 HA-mTRPC1-HA*) alone or in combination with unrelated control shRNA or shRNA targeting TRPC1. *D* and *E*, whole-cell measurements of Gn11 wild-type cells and of Gn11 cells transiently transfected with unrelated shRNA (*shRNA unrelated*) and with shRNA targeting TRPC1 (*shRNA anti-TRPC1*) with exemplary IV relationships before and during agonist stimulation with CCh in standard bath solution and in 10 mM Ca^{2+} solution in the presence of carbachol (*D*). The *arrows* indicate the reversal potentials in Ca^{2+} solution. *E*, shown is analysis of the respective calcium permeabilities. *F*, shown is current density analysis of Gn11 cells, Gn11 cells expressing unrelated shRNA, shRNA targeting TRPC1 or TRPC5, and Gn11 cells co-expressing shRNA targeting TRPC1 and TRPC5 or TRPC1, TRPC5, and TRPC6. Outward current densities at +60 mV are displayed, and basal current densities before agonist stimulation with carbachol are subtracted. Significant differences in comparison to wild-type, unrelated, and TRPC1 knockdown Gn11 cells are highlighted by an *asterisk*. *Numbers over the bars* indicate the number of cells measured. *G*, shown is analysis of fluorescence measurements of the basal cytosolic-free calcium concentrations $[Ca^{2+}]_i$ of fura-2-loaded Gn11 wild-type cells and of Gn11 cells stably expressing unrelated shRNA or shRNA against TRPC1 (TRPC1 knockdown). The *numbers over the bars* indicate the numbers of measured cells from four to six independent experiments. *H*, shown are exemplary time courses of two individual experiments with 12 fura-2-loaded control or TRPC1 knockdown Gn11 cells each are displayed. Time courses of the 12 cells are averaged. Changes of $[Ca^{2+}]_i$ in fura-2-loaded Gn11 cells were monitored after store depletion by 10 μM cyclopiazonic acid (*CPA*) in calcium-free, EGTA-buffered bath solution. Calcium influx after store depletion was induced by the addition of 2 mM Ca^{2+}. Application of 10 μM Gd^{3+} is displayed. *I*, shown are maximal increases of $[Ca^{2+}]_i$ during store depletion, and maximal calcium $[Ca^{2+}]_i$ answers after the readdition of 2 mM Ca^{2+} (*J*) are shown. Basal $[Ca^{2+}]_i$ was subtracted. The *first number over the bars* indicates the number of cells measured, and the *second number* indicates the number of independent experiments. *, $p < 0.05$; **, $p < 0.01$; ***, $p < 0.001$.

strongly suppresses TRPC1 expression. Next, whole-cell patch clamp measurements were performed with wild-type Gn11 cells and Gn11 cells expressing either unrelated control shRNA or shRNA directed against TRPC1. Current increases were induced by application of 100 μM carbachol or 1 μM bradykinin (data not shown). Interestingly, transient (Fig. 3, *D* and *E*) as

well as stable overexpression of shRNA against TRPC1 (supplemental Fig. S5) resulted in a significantly increased calcium permeability indicating that endogenously expressed TRPC1 proteins also reduce the overall calcium permeability in Gn11 neurons.

To analyze the molecular identity of the carbachol-induced cation currents in Gn11 cells, we performed additional whole-cell measurements with TRPC1 knockdown Gn11 cells transiently transfected with shRNA targeting murine TRPC5 and/or murine TRPC6. shRNA constructs targeting mouse TRPC5 and mouse TRPC6 were generated and tested for their efficiency performing quantitative qPCR and Western blot analysis (supplemental Fig. S6). In Gn11 cells stably expressing TRPC5 shRNA, the relative TRPC5 mRNA expression was markedly reduced (reduction of 76.6 ± 7.7% compared with WT Gn11 cells and 89.7 ± 3.4% compared with control cells expressing unrelated shRNA), whereas in Gn11 cells stably expressing TRPC6 shRNA, the relative TRPC6 mRNA expression was reduced to a smaller extent (reduction of relative mRNA expression of 54.3 ± 21.9% compared with WT Gn11 cells and 77.8 ± 10.6% compared with control cells expressing unrelated shRNA). However, in performing qPCR analysis we observed that TRPC6 mRNA expression levels are very low, close to the detection limit. Therefore, we performed Western blot analysis with CHO-K1 cells stably overexpressing HA-tagged mouse TRPC6 to monitor TRPC6 expression on the protein level. Co-expression of shRNA against TRPC6 markedly reduced TRPC6 expression (supplemental Fig. S6C), indicating that the generated shRNA against TRPC6 is effective. shRNA against TRPC5 or TRPC6 had no effect on the TRPC expression profile of Gn11 cells (data not shown). Interestingly, knockdown of TRPC1 resulted in a minor insignificant decrease of outward currents, whereas shRNA targeting TRPC5 caused a significant suppression of carbachol-induced cation currents (Fig. 3*F*). Knockdown of TRPC1 and TRPC5 resulted in a similar current reduction. Additional shRNA targeting of TRPC6 had no additional effect, indicating that TRPC6 is not relevant for carbachol-induced cation currents in Gn11 cells. Furthermore, TRPC2, which is mainly expressed in the vomeronasal organ, did not participate in receptor-operated cation currents. These results indicate that in Gn11 neuron receptor-operated cation currents are mainly mediated by heteromeric TRPC1 and TRPC5 channel complexes. Furthermore, these results strongly suggest that endogenous TRPC1 in Gn11 neurons is not able to form functional homomeric receptor-operated cation channel complexes.

To analyze the impact of calcium permeability on the global free intracellular calcium concentration ($[Ca^{2+}]_i$), Gn11 neurons were loaded with the fluorescent dye fura-2, and $[Ca^{2+}]_i$ was determined. We observed that $[Ca^{2+}]_i$ was significantly increased by 51.6 ± 9.2 nM when TRPC1 knockdown and control cells were compared (Fig. 3*G*), thus supporting the notion that TRPC1 is a regulator of the intracellular calcium concentration.

Because TRPC1 is regarded as a key player for store-operated calcium influx (8–10), we monitored changes of $[Ca^{2+}]_i$ in fura-2-loaded Gn11 neurons after performing established maneuvers to assess store-operated calcium entry. After store depletion in a calcium-free bath solution by 10 μM cyclopiazonic acid, an inhibitor of calcium ATPases in intracellular calcium stores, for more than 10 min, 2 mM Ca^{2+} was added to the bath and resulted in a rapid calcium influx. The calcium release component did not differ between TRPC1 knockdown and control cells (Fig. 3, *H* and *I*), and subsequent store-operated calcium influx was also not different (Fig. 3*J*). The addition of Gd^{3+} at the end of the procedure led to a decrease of $[Ca^{2+}]_i$ in both cases. These findings strongly suggest that TRPC1 is not a relevant component of store-operated calcium channels in GnRH neurons.

TRPC1 Is Involved in Migration of GnRH Neurons—GnRH neurons originate from the olfactory bulb from where they migrate to the hypothalamus to fully differentiate and to lose their migratory properties during development. To shed light on the role of TRPC1 as a calcium suppressor in Gn11 neurons, which are immature and still have the ability to migrate, we performed scratch assays. Interestingly, TRPC1 knockdown cells showed significantly enhanced motility compared with wild-type and control cells (Fig. 4, *A* and *B*). This increased migratory property was independent of the concentration of fetal calf serum, and it could not be further increased by agonist stimulation with carbachol, bradykinin, or endothelin-1. Additionally, we examined cell proliferation (supplemental Fig. S7) and apoptosis (data not shown) as alternative explanations for the apparent increased motility of TRPC1 knockdown neurons in scratch assays. We did not observe any differences in cell proliferation between control shRNA-expressing Gn11 and TRPC1 knockdown cells. However, untransfected Gn11 wild-type cells exhibited a slight increase in cell proliferation. Furthermore, TRPC1 had no effect on apoptosis (data not shown).

Because polymerization and depolymerization of actin are important determinants of cell motility (26), we investigated the F-actin/G-actin ratio by quantification of Western blots of cellular fractions of filamentous actin (F-actin) *versus* free globular-actin (G-actin) (Fig. 4, *C* and *D*). Phalloidin, which prevents depolymerization of F-actin, and cytochalasin D, which binds to G actin and prevents polymerization, were used as positive controls for F- and G-actin, respectively. Although there were no significant differences between F- and G-actin fractions in Gn11 and in control cells, TRPC1 knockdown cells showed a significantly increased G-actin fraction demonstrating that the enhanced motility of TRPC1 knockdown neurons is associated with a marked reorganization of the actin cytoskeleton. Taken together, these results suggest that TRPC1 knockdown cells exhibiting increased cytosolic calcium concentrations show increased cell motility, pointing to a specific role of TRPC1 for the migration of Gn11 neurons.

Moreover, performing time lapse videomicroscopy, we noted that TRPC1 knockdown and control Gn11 neurons significantly differed in terms of specific migratory properties like distance covered, migration speed, and directionality. TRPC1 knockdown cells changed direction less frequently, thereby covering a greater effective distance from start to end. Additionally, these cells moved with a higher speed, thus traveling a greater total distance, *e.g.* path length (Fig. 4, *E* and *F*). Additionally, the ratio of the total path length and the effective distance covered was decreased in TRPC1 knockdown cells, sug-

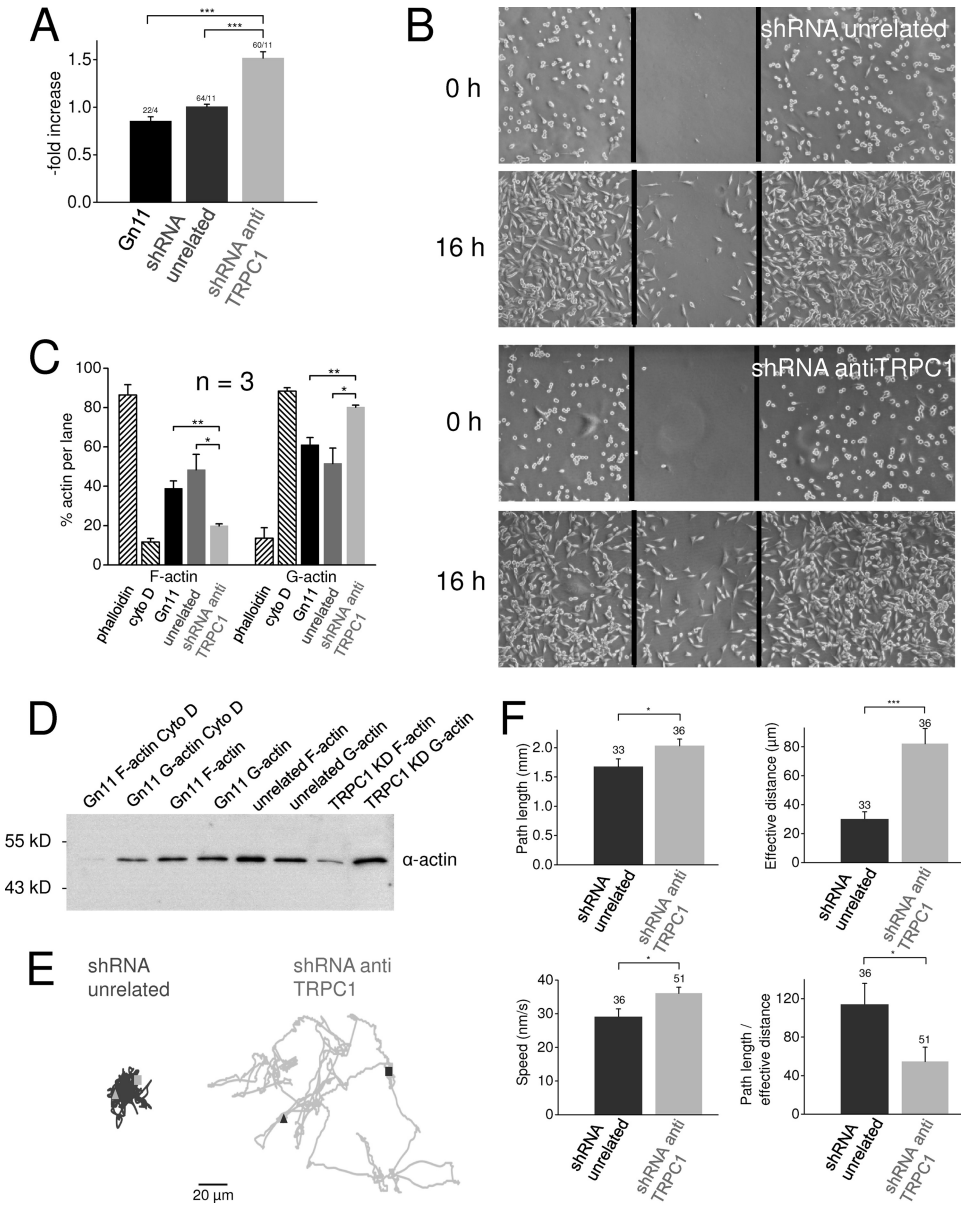

FIGURE 4. **TRPC1 reduces migration and motility of GnRH neurons.** *A*, shown is analysis of scratch assays with wild-type Gn11 cells and with Gn11 cells stably expressing unrelated shRNA or shRNA against TRPC1. *B*, a representative illustration of the migratory behavior of Gn11 cell lines in scratch assay right after scratch and after 16 h is shown. The *black lines* indicate the scratch performed with a yellow pipette tip. *C* and *D*, shown is analysis of the F-actin/G-actin assay with phalloidin as a positive control for F-actin, preventing F-actin depolymerization, and with cytochalasin D (*cyto D*) as a positive control for G-actin, preventing G-actin polymerization. *D*, a representative Western blot is displayed. *E* and *F*, translocation analysis of migrating Gn11 neurons with time laps movies is shown. *E*, exemplary trajectories of unrelated shRNA and shRNA against TRPC1 expressing Gn11 cells are shown. The *triangles* display the start, and the *squares* indicate the end of the movement. *F*, shown are the analysis of total path length, effective distance from start to end, speed, and the quotient between the total path length, and the effective distance displaying the degree of changes of direction. *Numbers over bars* indicate the number of measured cells. *, $p < 0.05$; **, $p < 0.01$; ***, $p < 0.001$.

gesting a lower degree of changes of direction. These findings provide strong evidence in favor of the concept that suppression of TRPC1 expression enhances neuronal motility.

DISCUSSION

The present study reveals that TRPC1 alone is not able to form functional homotetrameric, receptor-operated channels in heterologous expression systems. Instead, we made the observation that TRPC1 proteins are not only able to assemble to heteromeric receptor-operated channel complexes with TRPC4 and -5 (14, 25) but also form heteromeric complexes with all members of the diacylglycerol-sensitive subfamily TRPC3, -6, and -7, suggesting that TRPC1 is rather promiscuous in terms of heteromultimerization with other TRPC channels. Although interaction of TRPC1 with TRPC3/6/7 was previously not detected using co-immunoprecipitation or FRET analysis (27–29), we took advantage of a highly sensitive electrophysiological approach and found that TRPC1 functionally interacts with TRPC3, -6, or -7 to form receptor-operated channel complexes with distinct biophysical properties. Our data are in line with the findings of other groups showing heterotetramerization of TRPC1/3 or TRPC1/7 or of TRPC1/5/6 (14, 30–34).

To date there is still controversy about the issue as to whether TRPC1 is able to form functional homomeric channels. In our study the lack of agonist-, GTPγS-, or phosphatidylinositol 4,5-bisphosphate depletion-induced currents in TRPC1 overexpressing cells suggests that at least in the heterologous expression system employed by us, TRPC1 proteins *per se* are unable to form functional homomeric channels in the plasma membrane. This might be explained by their inability for homotetramerization or by intracellular localization of TRPC1 homomers, preventing insertion into the plasma membrane (35–37). However, at present we cannot rule out that homomeric TRPC1 channels are not gated by typical TRPC activators. However, we noted that amino acid exchanges from glutamate to glutamine at positions 581 and 582 in the putative pore-forming region of TRPC1 further reduced the calcium permeability of heteromeric channel complexes, indicating that TRPC1 is not an accessory (β) subunit of heteromeric channel complexes but that TRPC1 is involved in the formation of the channel pore.

There is still controversy about the role of TRPC1 for store-operated Ca^{2+} entry. Our previous studies with vascular smooth muscle cells of TRPC1 gene-deficient mice showed that TRPC1 is not involved in SOC (11). Likewise, Potier *et al.* (38) showed that SOC in vascular smooth muscle cells was independent of TRPC1 but was mediated by STIM1 and OraiI. So far, the role of TRPC1 for SOC in neurons is largely unknown. Applying an established store-depletion protocol, we did not observe an involvement of TRPC1 in SOC in Gn11 neurons. However, it was shown recently that TRPC1 is involved in SOC-dependent migration in transformed renal epithelial cells (MDCK-F cells) as a model to study tumor cell migration (39). Interestingly, Fabian *et al.* (39, 40) demonstrated that knockdown of TRPC1 by shRNA in MDCK-F cells resulted in a decrease of cytosolic $[Ca^{2+}]_i$ thereby impairing motility and directed migration. These findings contrast with our results but might be explained by different cell systems used and by a different TRPC channel expression levels of renal epithelial cells compared with neurons.

In this study Gn11 neurons were chosen as a model to study the cell physiological role of TRPC1 because of their pronounced TRPC1 expression. Furthermore, mRNA analysis revealed expression of TRPC2, -5, and -6 at lower levels. However, Gn11 cells were previously described to express all TRPC subtypes by immunochemistry (41), but recently the same group only detected TRPC1, -2, and -5 in these cells by mRNA analysis (42). Regarding the extraordinarily high expression level of TRPC1 and the select expression profile of other TRPC subtypes, Gn11 cells turned out to be an excellent model to study TRPC1 heteromers. Because Strübing *et al.* (14) had shown that heteromeric channel complexes consisting of TRPC4/5–3/6 can only assemble in the presence of TRPC1 and occur only in the embryonic brain during development but not in the adult brain, it was very likely that heteromeric TRPC channel complexes also occur in Gn11 neurons derived from embryonic brain. We could verify our experimental data obtained by expression of recombinant TRPC1 in a heterologous expression system by performing knockdown of TRPC1 in Gn11 neurons by an shRNA approach that did not impinge on the expression profile of other TRPC channels. Interestingly, TRPC1 knockdown Gn11 cells showed a significantly increased calcium permeability supporting the notion that endogenously expressed TRPC1 likewise functions as a suppressor of calcium permeability.

Ariano *et al.* (42) recently showed that TRPC channels are involved in calcium-dependent migration of Gn11 neurons. Here we identified TRPC1 as a specific regulator of the free cytosolic calcium concentration in Gn11 neurons controlling neuronal migration. Specific knockdown of TRPC1 in Gn11 cells resulted in increased $[Ca^{2+}]_i$ and in enhanced motility verified with three different approaches; 1) scratch assay, 2) time lapse microscopy, 3) determination of the G-actin/F-actin ratio. Although Ariano *et al.* (42) used unspecific TRP channel blockers like SKF96365 and La^{3+} and an antibody against the predicted pore-forming region of TRPC1, we performed specific down-regulation of TRPC1. Using the TRPC1 antibody to deactivate TRPC1, Ariano *et al.* (42) reduced the migration of Gn11 cells, which is contrary to our findings with knockdown of TRPC1 by shRNA. These conflicting results might be explained by a blockade of all heteromeric TRPC1 containing channels by the antibody thus resulting in decreased calcium influx and reduced calcium-dependent cell motility. Our knockdown approach by specific shRNAs ensured that other TRPC protein subtypes can still form functional channels allowing for calcium influx. Consequently, calcium influx was not impaired, and calcium permeability and free cytosolic $[Ca^{2+}]_i$ were increased. However, in line with Ariano *et al.* (42), we did not observe any effect of TRPC1 on proliferation.

Zaninetti *et al.* (43) have demonstrated that migration of Gn11 cells is dependent on calcineurin and nuclear factor of activated T-cells (NFAT). Therefore, we propose the following pathway. Down-regulation of TRPC1 in Gn11 cells increases the calcium permeability leading to a rise in cytosolic $[Ca^{2+}]_i$, thereby activating calmodulin, which subsequently activates calcineurin. Calcineurin in turn dephosphorylates nuclear factor of activated T-cells and induces translocation into the nucleus, thereby enhancing the transcription of genes pertinent to increased cell migration.

To summarize, our results provide several lines of evidence to support the new concept that in immortalized immature GnRH neurons TRPC1 suppress neuronal migration, thus highlighting a novel regulatory mechanism based on the formation of heteromeric TRPC channel complexes with reduced calcium permeability.

Acknowledgments—We thank Eva Braun, Ernst Bernges, Elisabeth Topoll, and Joanna Zaisserer for excellent technical assistance. We are grateful to Sally Radovick and Davide Lovisolo for providing Gn11 cells. We thank Alexander Dietrich and Meike Fahlbusch for supplying and cloning HA-mTRPC1-HA cDNA and Hermann Kalwa for assistance in the design of shRNA constructs. We are indebted to Alexander Liebstein (Zeiss) who made the AxioVision software available to us and to Christoph Klingner for initial help with time lapse microscopy.

REFERENCES

1. Hofmann, T., Obukhov, A. G., Schaefer, M., Harteneck, C., Gudermann, T., and Schultz, G. (1999) Direct activation of human TRPC6 and TRPC3 channels by diacylglycerol. *Nature* **397,** 259–263
2. Salido, G. M., Sage, S. O., and Rosado, J. A. (2009) TRPC channels and

store-operated Ca^{2+} entry. *Biochim. Biophys. Acta* **1793,** 223–230
3. Wu, L. J., Sweet, T. B., and Clapham, D. E. (2010) International union of basic and clinical pharmacology. LXXVI. Current progress in the mammalian TRP ion channel family. *Pharmacol. Rev.* **62,** 381–404
4. Bollimuntha, S., Selvaraj, S., and Singh, B. B. (2011) Emerging roles of canonical TRP channels in neuronal function. *Adv. Exp. Med. Biol.* **704,** 573–593
5. Cui, K., and Yuan, X. (2007) in *TRP Ion Channel Function in Sensory Transduction and Cellular Signaling Cascades* (Liedke, W. B., and Heller, S., eds) Chapter 4, CRC Press, Boca Raton, FL
6. Selvaraj, S., Sun, Y., and Singh, B. B. (2010) TRPC channels and their implication in neurological diseases. *CNS Neurol. Disord. Drug Targets* **9,** 94–104
7. Maroto, R., Raso, A., Wood, T. G., Kurosky, A., Martinac, B., and Hamill, O. P. (2005) TRPC1 forms the stretch-activated cation channel in vertebrate cells. *Nat. Cell Biol.* **7,** 179–185
8. Beech, D. J. (2005) TRPC1. Store-operated channel and more. *Pflugers Arch.* **451,** 53–60
9. Ambudkar, I. S., Ong, H. L., Liu, X., Bandyopadhyay, B. C., Bandyopadhyay, B., and Cheng, K. T. (2007) TRPC1. The link between functionally distinct store-operated calcium channels. *Cell Calcium* **42,** 213–223
10. Yuan, J. P., Kim, M. S., Zeng, W., Shin, D. M., Huang, G., Worley, P. F., and Muallem, S. (2009) TRPC channels as STIM1-regulated SOCs. *Channels* **3,** 221–225
11. Dietrich, A., Kalwa, H., Storch, U., Mederos y Schnitzler, M., Salanova, B., Pinkenburg, O., Dubrovska, G., Essin, K., Gollasch, M., Birnbaumer, L., and Gudermann, T. (2007) Pressure-induced and store-operated cation influx in vascular smooth muscle cells is independent of TRPC1. *Pflugers Arch.* **455,** 465–477
12. Varga-Szabo, D., Authi, K. S., Braun, A., Bender, M., Ambily, A., Hassock, S. R., Gudermann, T., Dietrich, A., and Nieswandt, B. (2008) Store-operated Ca^{2+} entry in platelets occurs independently of transient receptor potential (TRP) C1. *Pflugers Arch.* **457,** 377–387
13. Rychkov, G., and Barritt, G. J. (2007) TRPC1 Ca^{2+}-permeable channels in animal cells. *Handb. Exp. Pharmacol.* **179,** 23–52
14. Strübing, C., Krapivinsky, G., Krapivinsky, L., and Clapham, D. E. (2003) Formation of novel TRPC channels by complex subunit interactions in embryonic brain. *J. Biol. Chem.* **278,** 39014–39019
15. Radovick, S., Wray, S., Lee, E., Nicols, D. K., Nakayama, Y., Weintraub, B. D., Westphal, H., Cutler, G. B., Jr., and Wondisford, F. E. (1991) Migratory arrest of gonadotropin-releasing hormone neurons in transgenic mice. *Proc. Natl. Acad. Sci. U. S. A.* **88,** 3402–3406
16. Brummelkamp, T. R., Bernards, R., and Agami, R. (2002) A system for stable expression of short interfering RNAs in mammalian cells. *Science* **296,** 550–553
17. Reynolds, A., Leake, D., Boese, Q., Scaringe, S., Marshall, W. S., and Khvorova, A. (2004) Rational siRNA design for RNA interference. *Nat. Biotechnol.* **22,** 326–330
18. Yiu, S. M., Wong, P. W., Lam, T. W., Mui, Y. C., Kung, H. F., Lin, M., and Cheung, Y. T. (2005) Filtering of ineffective siRNAs and improved siRNA design tool. *Bioinformatics* **21,** 144–151
19. Lewis, C. A. (1979) Ion concentration dependence of the reversal potential and the single channel conductance of ion channels at the frog neuromuscular junction. *J. Physiol.* **286,** 417–445
20. Grynkiewicz, G., Poenie, M., and Tsien, R. Y. (1985) A new generation of Ca^{2+} indicators with greatly improved fluorescence properties. *J. Biol. Chem.* **260,** 3440–3450
21. Dietrich, A., Mederos y Schnitzler, M., Emmel, J., Kalwa, H., Hofmann, T., and Gudermann, T. (2003) *N*-Linked protein glycosylation is a major determinant for basal TRPC3 and TRPC6 channel activity. *J. Biol. Chem.* **278,** 47842–47852
22. Tang, D. D., Zhang, W., and Gunst, S. J. (2005) The adapter protein CrkII regulates neuronal Wiskott-Aldrich syndrome protein, actin polymerization, and tension development during contractile stimulation of smooth muscle. *J. Biol. Chem.* **280,** 23380–23389
23. Trebak, M., Lemonnier, L., DeHaven, W. I., Wedel, B. J., Bird, G. S., and Putney, J. W., Jr. (2009) Complex functions of phosphatidylinositol 4,5-bisphosphate in regulation of TRPC5 cation channels. *Pflugers Arch.* **457,** 757–769
24. Otsuguro, K., Tang, J., Tang, Y., Xiao, R., Freichel, M., Tsvilovskyy, V., Ito, S., Flockerzi, V., Zhu, M. X., and Zholos, A. V. (2008) Isoform-specific inhibition of TRPC4 channel by phosphatidylinositol 4,5-bisphosphate. *J. Biol. Chem.* **283,** 10026–10036
25. Strübing, C., Krapivinsky, G., Krapivinsky, L., and Clapham, D. E. (2001) TRPC1 and TRPC5 form a novel cation channel in mammalian brain. *Neuron* **29,** 645–655
26. Machesky, L. M., and Insall, R. H. (1999) Signaling to actin dynamics. *J. Cell Biol.* **146,** 267–272
27. Hofmann, T., Schaefer, M., Schultz, G., and Gudermann, T. (2002) Subunit composition of mammalian transient receptor potential channels in living cells. *Proc. Natl. Acad. Sci. U. S. A.* **99,** 7461–7466
28. Goel, M., Sinkins, W. G., and Schilling, W. P. (2002) Selective association of TRPC channel subunits in rat brain synaptosomes. *J. Biol. Chem.* **277,** 48303–48310
29. Brownlow, S. L., and Sage, S. O. (2005) Transient receptor potential protein subunit assembly and membrane distribution in human platelets. *Thromb. Haemost.* **94,** 839–845
30. Lintschinger, B., Balzer-Geldsetzer, M., Baskaran, T., Graier, W. F., Romanin, C., Zhu, M. X., and Groschner, K. (2000) Coassembly of Trp1 and Trp3 proteins generates diacylglycerol- and Ca^{2+}-sensitive cation channels. *J. Biol. Chem.* **275,** 27799–27805
31. Liu, X., Bandyopadhyay, B. C., Singh, B. B., Groschner, K., and Ambudkar, I. S. (2005) Molecular analysis of a store-operated and 2-acetyl-*sn*-glycerol-sensitive non-selective cation channel. Heteromeric assembly of TRPC1-TRPC3. *J. Biol. Chem.* **280,** 21600–21606
32. Zagranichnaya, T. K., Wu, X., and Villereal, M. L. (2005) Endogenous TRPC1, TRPC3, and TRPC7 proteins combine to form native store-operated channels in HEK-293 cells. *J. Biol. Chem.* **280,** 29559–29569
33. Wu, X., Zagranichnaya, T. K., Gurda, G. T., Eves, E. M., and Villereal, M. L. (2004) A TRPC1/TRPC3-mediated increase in store-operated calcium entry is required for differentiation of H19–7 hippocampal neuronal cells. *J. Biol. Chem.* **279,** 43392–43402
34. Saleh, S. N., Albert, A. P., and Large, W. A. (2009) Activation of native TRPC1/C5/C6 channels by endothelin-1 is mediated by both PIP_3 and PIP_2 in rabbit coronary artery myocytes. *J. Physiol.* **587,** 5361–5375
35. Berbey, C., Weiss, N., Legrand, C., and Allard, B. (2009) Transient receptor potential canonical type 1 (TRPC1) operates as a sarcoplasmic reticulum calcium leak channel in skeletal muscle. *J. Biol. Chem.* **284,** 36387–36394
36. Wang, W., O'Connell, B., Dykeman, R., Sakai, T., Delporte, C., Swaim, W., Zhu, X., Birnbaumer, L., and Ambudkar, I. S. (1999) Cloning of Trp1β isoform from rat brain. Immunodetection and localization of the endogenous Trp1 protein. *Am. J. Physiol.* **276,** C969–C979
37. Uehara, K. (2005) Localization of TRPC1 channel in the sinus endothelial cells of rat spleen. *Histochem. Cell Biol.* **123,** 347–356
38. Potier, M., Gonzalez, J. C., Motiani, R. K., Abdullaev, I. F., Bisaillon, J. M., Singer, H. A., and Trebak, M. (2009) Evidence for STIM1- and Orai1-dependent store-operated calcium influx through ICRAC in vascular smooth muscle cells. Role in proliferation and migration. *FASEB J.* **23,** 2425–2437
39. Fabian, A., Fortmann, T., Dieterich, P., Riethmüller, C., Schön, P., Mally, S., Nilius, B., and Schwab, A. (2008) TRPC1 channels regulate directionality of migrating cells. *Pflugers Arch.* **457,** 475–484
40. Fabian, A., Fortmann, T., Bulk, E., Bomben, V. C., Sontheimer, H., and Schwab, A. (2011) Chemotaxis of MDCK-F cells toward fibroblast growth factor-2 depends on transient receptor potential canonical channel 1. *Pflugers Arch.* **461,** 295–306
41. Dalmazzo, S., Antoniotti, S., Ariano, P., Gilardino, A., and Lovisolo, D. (2008) Expression and localization of TRPC channels in immortalised GnRH neurons. *Brain Res.* **1230,** 27–36
42. Ariano, P., Dalmazzo, S., Owsianik, G., Nilius, B., and Lovisolo, D. (2011) TRPC channels are involved in calcium-dependent migration and proliferation in immortalized GnRH neurons. *Cell Calcium* **49,** 387–394
43. Zaninetti, R., Tacchi, S., Erriquez, J., Distasi, C., Maggi, R., Cariboni, A., Condorelli, F., Canonico, P. L., and Genazzani, A. A. (2008) Calcineurin primes immature gonadotropin-releasing hormone-secreting neuroendocrine cells for migration. *Mol. Endocrinol.* **22,** 729–736